

Comparison of Thermal Fatigue Performance of SAC105 (Sn-1.0Ag-0.5Cu), Sn-3.5Ag, and SAC305 (Sn-3.0Ag-0.5Cu) BGA Components with SAC305 Solder Paste

Gregory Henshall,
Hewlett-Packard Co.
Palo Alto, CA
Jasbir Bath, Bath Technical Consultancy
Sundar Sethuraman, Jabil
David Geiger, Flextronics International
Ahmer Syed, Amkor
M.J. Lee, Xilinx
Keith Newman and Livia Hu, Sun Microsystems
Dong Hyun Kim and Weidong Xie, Cisco Systems
Wade Eagar and Jack Waldvogel, Motorola

Abstract

Many BGA and CSP component suppliers have begun shipment of components with a variety of “second generation” Pb-free solder ball alloys. Much of the motivation for the alloy changes has been to improve mechanical shock resistance. Several publications have established the improved performance of such 2nd level BGA/CSP sphere alloys; however, much less has been published regarding the thermal fatigue resistance of components with these new Pb-free ball alloys. As these components and alloys become mainstream, their use in situations where thermal fatigue resistance is critical to product life will become an important consideration. Therefore, an understanding of thermal fatigue performance for new alloys is necessary for OEM/ EMS/ ODM companies to make design and procurement decisions, and for component suppliers to ensure the reliability of their products under a range of field use conditions.

In this study, the thermal fatigue performance under accelerated test conditions is compared for three common BGA ball alloys: SAC105, Sn-3.5Ag, and SAC305 as a control. Accelerated thermal cycle (ATC) testing was performed using 676 PBGA components with 1.0 mm pitch and electrolytic Ni/Au finished component pads. These components were assembled to high-temperature rated Cu-OSP coated printed circuit boards using SAC 305 solder paste, which represents one of the most common assembly practices in industry today. ATC testing was performed using the IPC-9701A TC1 condition of 0/100°C with 10-minute dwells (nominal); 3 different failure criteria were used in constructing the Weibull failure curves. The data indicate that SAC105 has the lowest thermal fatigue resistance among the alloys tested, with Sn-3.5Ag and SAC 305 having similar and superior performance. The impact of failure criterion on the Weibull curves is also presented. The implications of these findings and areas for further study are discussed.

Introduction

Several publications [1-7] have demonstrated improved mechanical shock fracture resistance for a variety of “second generation” Pb-free solder ball alloys. A number of BGA/CSP component suppliers are now shipping devices that use these new solder alloys. However, iNEMI has identified the thermal fatigue resistance of the new Pb-free ball alloys to be a major knowledge gap [8, 9]. In situations where thermal fatigue resistance is critical to product life, this knowledge gap creates a significant risk. One example is in memory devices, where low-Ag alloys are being introduced by some suppliers. As such devices begin use in the next generation Pb-free servers; thermal fatigue resistance is likely to be a concern due to their relatively large die and the demanding thermal environment. Therefore, an understanding of thermal fatigue performance for new alloys is necessary for OEMs to make design and procurement decisions, and for component suppliers to ensure the reliability of their products over a range of field use conditions.

Experimental Materials and Procedures

Test vehicle materials and assembly

Three BGA ball alloys of current industrial interest were investigated: Sn-1.0Ag-0.5Cu (SAC105), Sn-3.5Ag, and Sn-3.0Ag-0.5Cu (SAC305) as a control. Sn-3.5Ag is one alloy typically targeted for large BGA, while SAC105 is one alloy targeted for small BGAs and CSPs. SAC 305 solder paste was used in all cases to solder the packages to the test boards, which is the most common practice in industry today.

The test vehicle used in this study was leveraged from an earlier project by our “Industry Working Group,” as described by Bath et al. [10]. Thus, the board layout, PCB, and BGA package characteristics are the same as those reported earlier. Some key items of note are provided in Table 1.

Table 1. Test vehicle characteristics.

PCB	
Thickness	2.36 mm (0.093 in.)
Finish	High temp. Cu-OSP
No. Cu Layers	9
Pad dia.	0.4 mm
Solder mask dia.	0.55 mm
BGA Package	
Die size	17 x 17 mm
Package size	27 x 27 mm
Ball array	26 x 26
Ball pitch	1 mm
Ball dia.	0.6 mm
Pad type	SMD
Solder mask dia.	0.45 mm
Pad finish	Electrolytic Ni/Au

Three sets of boards were built to investigate the three different ball alloys. In each case, the peak reflow temperature was 240-243°C in order to achieve full mixing, given ball alloy liquidus temperatures of 219°C - 225°C and SAC305 paste liquidus of 219°C [11, 12]. The laser-cut stencil thickness was 125 μ m (0.005 in.) with 0.46 mm (0.018 in.) diameter openings.

Figure 1 shows the microstructure of a typical joint formed using the SAC105 ball and SAC305 paste. Full ball collapse and a homogeneous microstructure are evident. Given this homogeneity, the “mixed alloy composition calculator” of Pan [13] was used to estimate the final composition and liquidus temperature of the joints. These results are provided in Table 2. Note that these estimates do not include any Cu, Ni, or other elements dissolved into the joint from the soldering pads, and do not reflect the elemental composition of the intermetallic (IMC) layers at the solder pad interfaces. Table 2 indicates that the joint composition for the Sn-3.5Ag ball alloy alters only slightly due to the presence of SAC 305 paste, as expected. More importantly, this table shows that the SAC305 paste does not alter the overall joint composition by a significant amount for the SAC105 ball. Since the ball diameter is relatively large for these 1 mm pitch components, the SAC105 ball composition dominates so that the assembly with SAC305 paste changes the composition only by 0.1% Ag. Thus, the results of this study give a good indication of the behavior for the SAC105 ball alloy.

For the accelerated thermal cycle (ATC) test boards, all 6 locations (U1 to U6) were populated on the board. Paste printing, component placement and reflow were conducted with conventional SMT production equipment. The 10-zone convection reflow oven used an air atmosphere. The reflow profile incorporated a 65-70 s dwell above 217°C, a peak solder joint temperature of 240-243°C, and a maximum solder joint heating/cooling rate of 2.0/3.5°C/s.

After assembly, boards were X-ray inspected and daisy chains were tested for defects. Minor delamination was observed in 2 of 15 boards, without any associated solder joint defects or via damage. The delamination occurred during reflow due to excess moisture absorption in the circuit boards during prolonged storage. Following thermal cycle test completion, destructive analysis also indicated the presence of some solder non-wetting during initial board assembly that was not originally detected by X-ray examination. The non-wetting was again sourced to prolonged board storage, in this case resulting in degradation of the organic solderability preservative. This non-wetting was rare and did not appear to have negatively impacted the ATC results. The solder joint standoff heights after assembly typically ranged from approximately 0.42 mm (0.0165 in.) to 0.50 mm (0.0197 in.).

Five boards were fully populated and built for each ball alloy, yielding 30 package test samples per alloy. Unfortunately, equipment failure during thermal cycle testing limited some of the SAC305 component data recording. Sufficient data were gathered, however, particularly for the 500 Ω and hard open failure criteria, to allow comparison of the SAC305 control test to the “alternate” alloys.

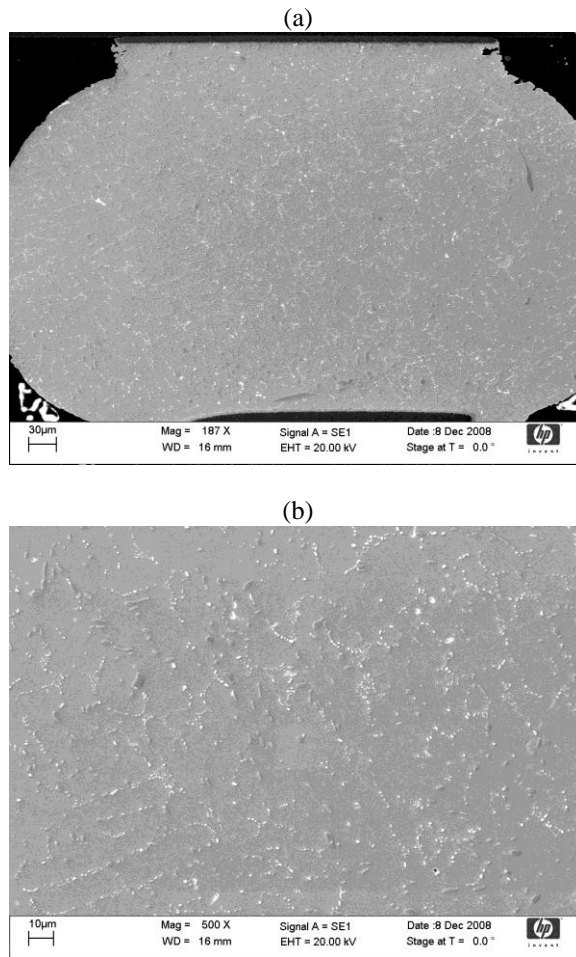


Figure 1. SEM micrographs of a typical joint formed using a SAC105 ball and SAC305 paste showing (a) ball collapse and overall homogeneity, and (b) detailed microstructure within a typical joint.

Table 2. Estimated solder joint composition and liquidus temperature for the BGA ball alloys soldered with SAC305 paste [13].

Ball Alloy	Calculated Final Joint Composition	Predicted Liquidus Temp. (°C)
SAC305	Sn-3.0Ag-0.5Cu	219
Sn-3.5Ag	Sn-3.46Ag-0.04Cu	221
SAC105	Sn-1.15Ag-0.5Cu	225

ATC Testing Procedure

The target ATC profile was IPC-9701A condition TC1: 0°C to 100°C with 10 minute ramps and dwells (40 minute total cycle time). The actual temperature profile is shown in Figure 2, which includes data from 6 different thermocouples attached to different test boards. The thermal profile was very uniform at different locations within the oven. The actual cycle was from -6°C to +104°C, for a ΔT of 110°C, with 10 minutes above 100°C, 9 minutes below 0°C, and a total cycle time of 51 minutes.

Solder joint interconnect integrity was monitored using one daisy-chain net for each package. Continuous in-situ monitoring of daisy-chain resistance was conducted throughout ATC testing. The data acquisition software “flagged” a daisy-chain net as failed using the IPC-9701A standard criterion of a 20% resistance rise. Since the resistance (R) is a function of temperature (T), measured R(T) values at any point during the test were compared against those measured on the first thermal cycle at an equivalent T. A “failure” was recorded once the following condition was met:

$$R(T) > 1.2 \cdot R_0(T) , \quad (1)$$

Where $R_0(T)$ represents the resistance measured during the first cycle at temperature T . This method compares the net resistance at all temperatures, not at a single reference temperature. For this study, the failure threshold was typically first exceeded during the ramp portion of the cycle, and not during either dwell.

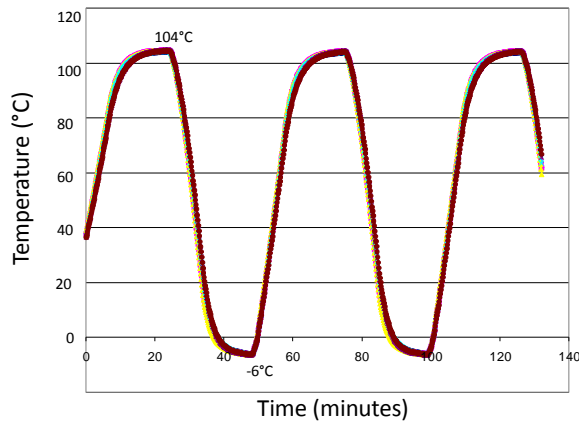


Figure 2. Thermal profile as measured on test boards at 6 different locations.

The in-situ monitoring equipment also allowed for evaluation of the number of cycles to failure using coarser failure criteria than the IPC-9701 standard. Thus, Weibull curves were also constructed using 500 Ω and “infinite” resistance (hard open) criteria in order to evaluate the impact of failure criterion on the reported thermal fatigue life of the joints. The nominal daisy-chain net resistance, R_0 , for the samples was approximately 2.5-5.0 Ω .

Failure Analysis

Two techniques were used to validate that thermal fatigue was the cause of the electrical failures. Dye stain analysis was used to establish complete solder joint failure. Following standard techniques, a concentrated red machinist’s dye was driven into existing cracks using ultrasonic agitation followed by drying of the dye. A mechanical testing machine was used to slowly bend the board and fully separate it from the packages. The presence of dye was detected using an optical stereo microscope.

The second technique, cross sectioning, was used to establish failure within the solder by thermal fatigue cracking. Standard metallographic techniques were used to grind and polish the samples, finishing with a colloidal silica polish that also provided a light etch. Regular and cross-polarized lighting were used to image the cross sections. In addition to optical analysis, scanning electron microscopy (SEM) also was used to investigate the microstructure of the joints. Secondary electron mode was used to image the cross sections.

Experimental Results

Impact of failure criterion

Figures 3 and 4 show the impact of the electrical resistance failure criterion on the solder joint life for the SAC105 and Sn-3.5Ag ball alloy joints. Data for the SAC305 control were sparse and are not shown here, though the trends in behavior were the same as for the other two alloys. The data in Figs. 3 and 4 show that the 20% resistance rise criterion gives a more sensitive measure of failure than the other two resistance levels. Differences in characteristic life, \square , between the 20% resistance rise and 500 Ω or hard open resistance criteria are typically 200 to 500 cycles, or about 3% to 10% of lifetime. The Weibull slopes, \square , for each set of data are fairly similar, with that for the 20% resistance rise being slightly lower at about 9.5 compared to the values of 12-14 for the 500 Ω and hard open criteria. The quality of the fits was excellent and nearly equivalent for all sets of data, with the correlation coefficient, \square , ranging from 0.97 to over 0.99. No systematic variation in \square was observed as a function of failure criterion.

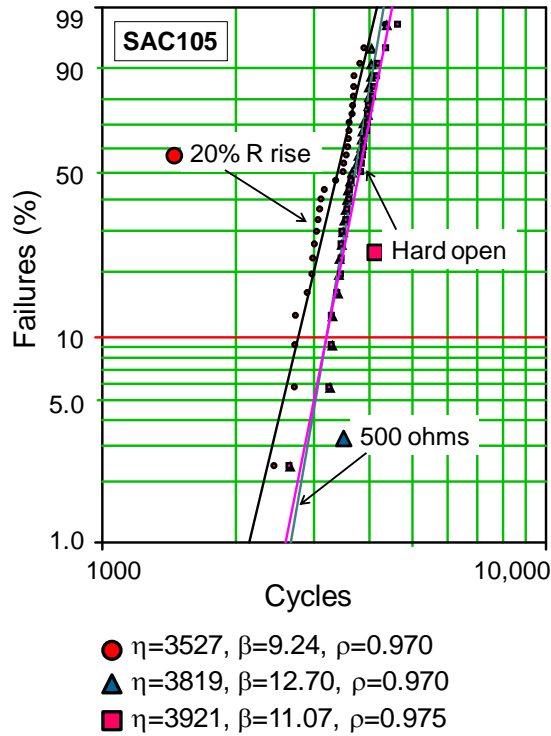


Figure 3. Weibull plots of failure life for the SAC105 ball alloy joints with SAC305 solder paste for three different electrical failure criteria.

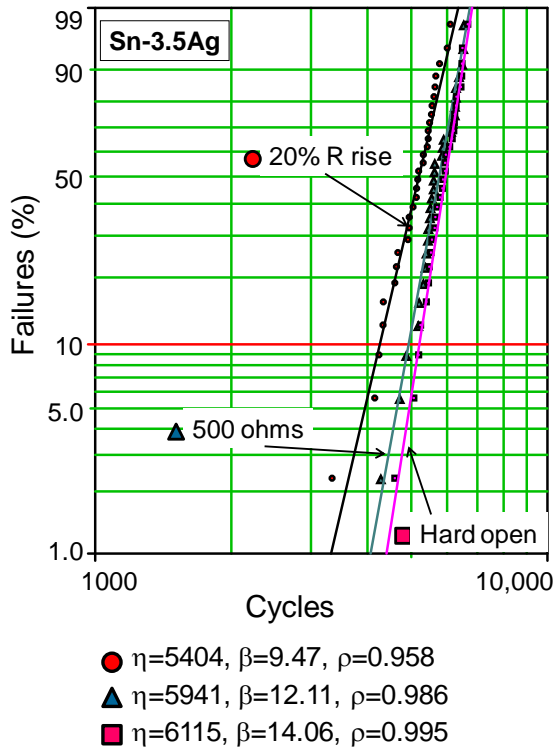


Figure 4. Weibull plots of failure life for the Sn-3.5Ag ball alloy joints with SAC305 solder paste for three different electrical failure criteria.

Impact of solder ball alloy

The impact of ball alloy on solder joint life is shown in Figures 5 – 7 for the three different failure criteria. These figures clearly show that BGAs with the SAC105 balls (soldered with SAC305 paste) have a lower accelerated thermal fatigue life compared to the higher Ag alloys. As expected, these data also show that the thermal fatigue life for SAC305 and Sn-3.5Ag balled BGAs are very similar for this package under the conditions tested. The similarity in ATC life between Sn-3.5 Ag and SAC 305/387/405 alloys has been observed previously by Yoon et al. [14]. The data also show that the rank ordering of the alloys is not affected by the choice of failure criterion. Keep in mind, however, that these results represent the behavior for the accelerated test conditions and for the components used in this study, and may or may not represent behavior for other package styles or under other thermal fatigue conditions, such as those of products in the field [15]. Further, the impact of BGA ball size, and thus the composition of the mixed joint, is not possible to determine from these test data.

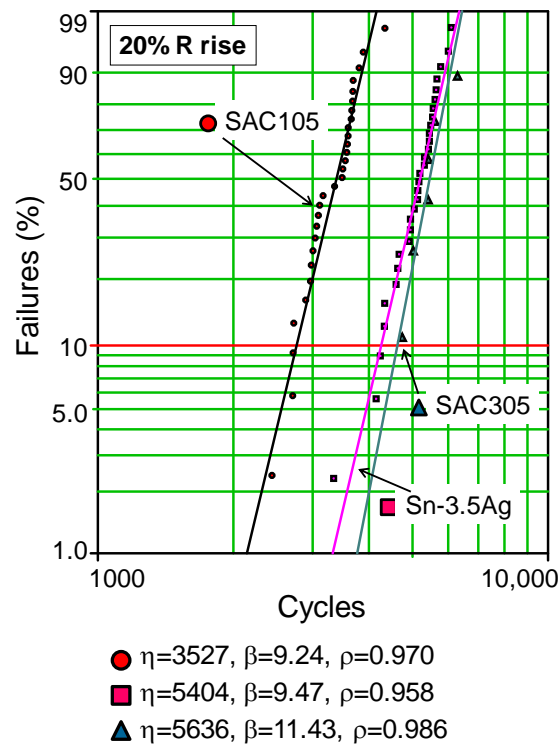


Figure 5. Weibull plots of failure life for the three different ball alloy joints using an electrical failure criterion of 20% resistance rise.

Table 3 compares the values of characteristic life, η , and estimated life at 1% failure for each alloy for each of the three failure criteria. Across all three failure criteria (20% R rise, 500 Ω , hard open), the characteristic lives for joints using the SAC105 ball are from 35% to 41% less than those of joints using Sn-3.5Ag or SAC305 solder balls. Similar differences are evident for the 1% failure life. There was no systematic correlation between ball alloy and Weibull slope across the three failure criteria.

Failure analysis

Confirmation that electrical failures were caused by thermal fatigue in the solder joints was established by removing samples from the chamber shortly after the first failures were detected and performing destructive analysis. Figure 8 shows the dye stain results for the Sn-3.5Ag ball alloy packages, demonstrating failure through the solder joints. As expected for this PBGA package, failures occurred near the die shadow, not at the corners of the component. Figure 9 shows the cross section results for SAC105 ball alloy joints. This micrograph clearly shows failure occurs by thermal fatigue crack propagation in the solder near the pad surface on the package side of the joint. It also appears that fatigue cracking in the SAC105 alloy may be occurring together with recrystallization near the crack, as shown in Fig. 10. Similar behavior was sometimes observed on the package side of the joint, where final failures typically occurred. Cracking at the recrystallized grain boundaries has been observed in SAC alloys by other investigators [16]. No evidence of pad cratering caused by thermal cycling was detected in the failure analyses.

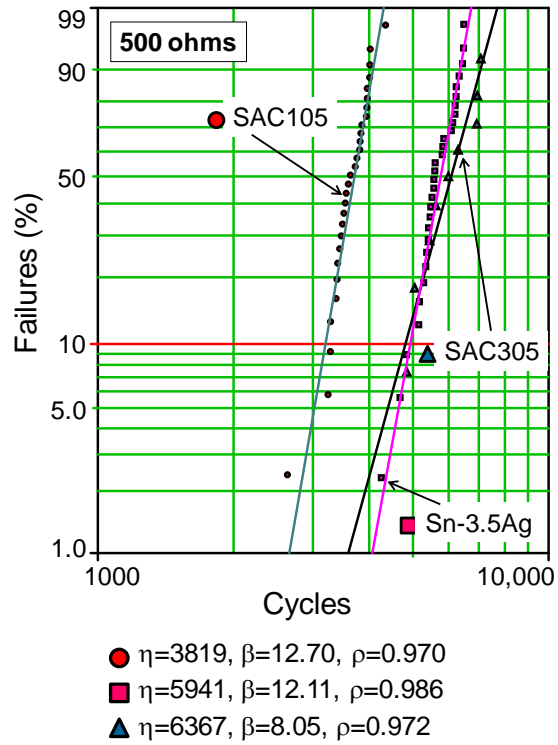


Figure 6. Weibull plots of failure life for the three different ball alloy joints using an electrical failure criterion of 500 Ω .

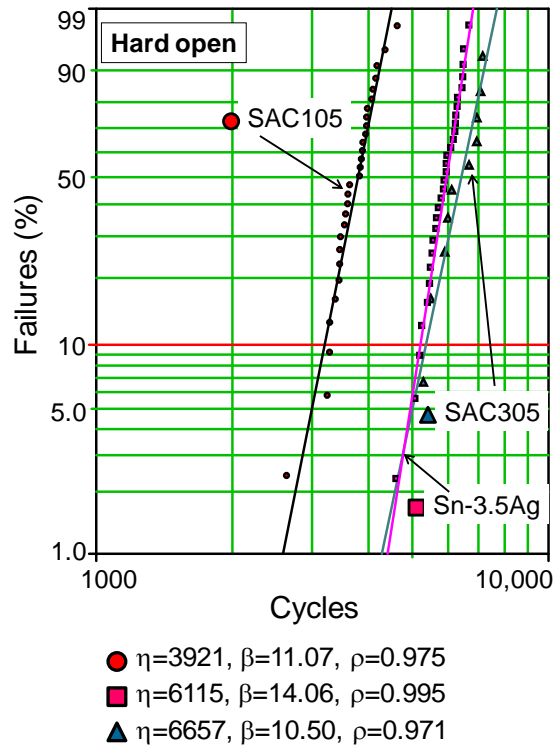


Figure 7. Weibull plots of failure life for the three different ball alloy joints using an electrical failure criterion of a hard open.

Table 3. Summary of data from the ATC testing.

Failure Criterion	Ball Alloy	1% Failure Life (cycles)	□ (cycles)	□ (slope)
20% R rise	SAC105	2140	3527	9.24
	Sn-3.5Ag	3320	5404	9.47
	SAC305	3760	5636	11.43
500 Ω	SAC105	2660	3819	12.70
	Sn-3.5Ag	4060	5941	12.11
	SAC305	3590	6367	8.05
Hard Open	SAC105	2590	3921	11.07
	Sn-3.5Ag	4410	6115	14.06
	SAC305	4280	6657	10.50

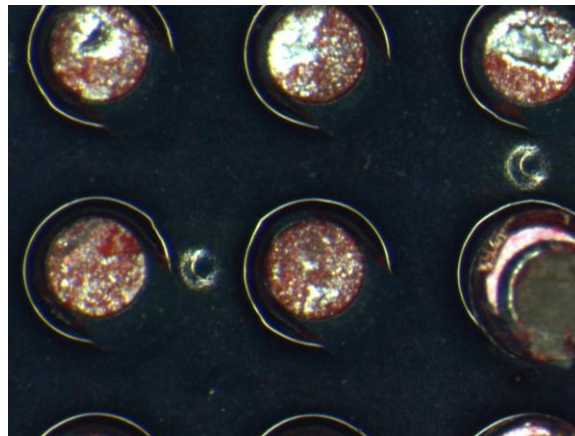


Figure 8. Results of dye stain analysis showing fully cracked solder joints. Sn-3.5Ag ball alloy package following 4628 thermal cycles.

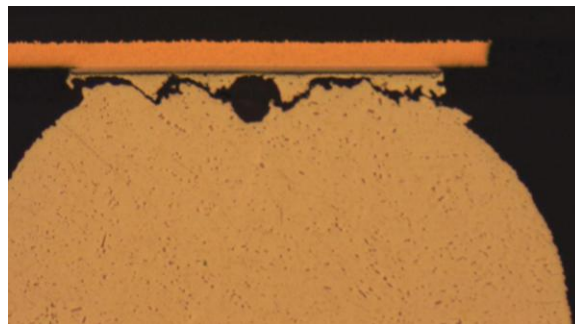


Figure 9. Cross section showing thermal fatigue crack through the solder joint near the package pad for a SAC105 ball alloy package following 4628 thermal cycles.

Further confirmation of thermal fatigue failures was performed after thermal cycling was complete (8150 cycles). For each alloy, the two packages failing last were used for dye stain and cross sectional analysis. In all cases, these analyses confirmed the failure mode to be the same as that observed for the early failures: thermal fatigue cracking in the joint near the package pad interface. Figure 11 provides an example for the SAC305 ball alloy package. These findings are consistent with our earlier study on SAC soldered joints [10].

Discussion

The results presented in the previous section clearly show that BGA solder joints made using SAC105 balls with no dopants perform significantly worse than high Ag alloys under the ATC test conditions investigated. This finding is consistent with that of Terashima [17], who found a systematic degradation in accelerated thermal fatigue performance as the Ag content of SAC alloys decreased from 4% to 1%.

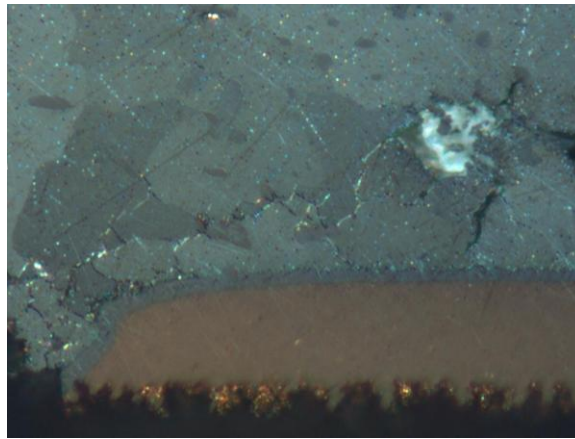


Figure 10. Cross-polarized light micrograph showing apparent recrystallization and grain-boundary cracking near the PCB pad in a SAC105 ball alloy solder joint subjected to 4628 thermal cycles.

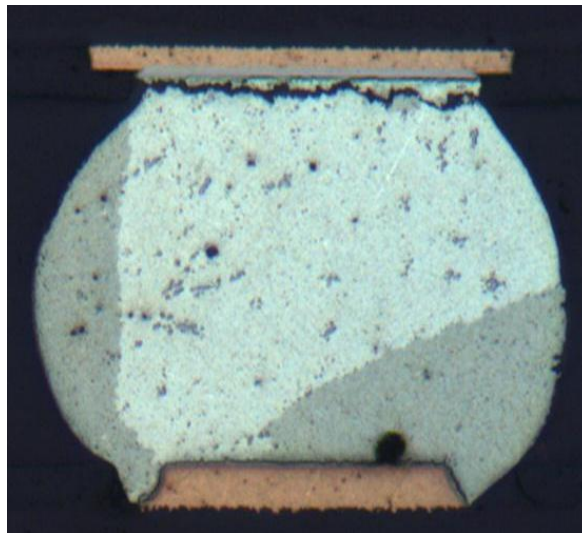


Figure 11. Cross-polarized light micrograph showing thermal fatigue cracking through the solder joint near the package pad for a SAC305 ball alloy package following 8151 thermal cycles.

Of course, the fact that the SAC105 ball alloy joints perform worse than the high Ag alloys (e.g. SAC305 and Sn-3.5Ag) under accelerated conditions does not necessarily mean that their performance isn't good enough for many applications. The characteristic life of 3527 to 3921 cycles under the accelerated conditions used in this experiment is probably sufficient for many applications.

One benchmark that would shed some light on the adequacy of these joints in thermal fatigue would be to compare the SAC105 results with those of eutectic Sn-Pb joints. Unfortunately, for the present study we did not have sufficient materials (boards and packages) to run such a control. However, the results of Bath et al. from the earlier study [10] can be examined. For the same *nominal* test vehicle and *nominal* thermal cycle profile, the 676 PBGA package using eutectic Sn-Pb ball and paste gave $\bar{n} = 5971$ cycles, considerably higher than the values measured in the present study for the SAC105 ball / SAC305 paste joints. Bath et al. also measured $\bar{n} = 5797$ cycles for joints made using a SAC405 ball and SAC396 solder paste. This value is similar to those measured for SAC305 joints in the present study. Thus, this direct comparison could suggest that SAC105 joints perform worse than Sn-Pb joints, implying risk in using the SAC105 solder ball in applications where thermal fatigue failure is a concern. However, many studies have shown a large difference between the behavior of eutectic Sn-Pb joints and SAC joints for 0-100°C conditions [15, 18], often up to a factor of two or more. The previous study by Bath et al. [10] showed similar performance for SAC and Sn-Pb joints. The reason for this similarity is not clearly understood. Thus, further studies directly comparing the thermal fatigue performance of Sn-Pb joints and those made using low Ag ball alloys is recommended in order to directly benchmark the Pb-free alloys against the industry's historical solution.

It should also be recognized that the above comparisons are based on accelerated test conditions. Because the creep behavior of solder alloys is highly temperature dependent, implying temperature dependent acceleration factors, and since field conditions can be more benign, it is entirely possible that solder joints formed using low Ag alloys might pass field level reliability requirements for most cases.

Figures 3 and 4 demonstrate the impact of the electrical failure criterion on the measured thermal fatigue life. The 20% resistance rise criterion suggested by IPC-9701A gives a more sensitive measure of failure than high resistance criteria, but may result in a somewhat wider failure distribution. The 500 ohm and hard open criteria give very similar lifetimes, suggesting that once high resistances occur, hard open failures are imminent. Selection of the proper criterion may depend upon the purpose of the test. The 20% resistance rise is probably most useful for OEMs trying to establish the first point at which intermittent signals, logic problems, etc., begin to occur for a particular package/design; this condition defines failure for many products. Thus, the 20% resistance rise criterion gives a conservative and meaningful measure of thermal fatigue failure. On the other hand, the lower scatter and reduced sensitivity to experimental execution provided by the 500 Ω and hard open criteria may be better suited for studies of basic material behavior (such as the current study), where a high confidence failure measure and low scatter in the Weibull curve benefit efforts to compare materials. This impact of failure criterion on measured fatigue life might also be dependent on the component type tested and the actual fatigue life. Other data [19] suggest no significant difference in fatigue life for these criteria on a smaller wafer level package which failed below 1000 cycles, as opposed to the failure lives of 3000 – 6000 cycles in this study.

Based on the results of the present study, several areas for future work on the thermal fatigue resistance of new Pb-free alloys are apparent. Generally, these findings support those published by iNEMI [8]. These include:

- Benchmarking the results for low Ag alloys against those for eutectic Sn-Pb joints within the same study.
- Assessing the impact of dopants such as Ni, Bi, etc. Some evidence exists that dopants could have a significant impact on thermal fatigue resistance of low Ag alloys [20].
- Assessing the impact of surface finishes, which may also add extra elements, such as Ni, into the joint.
- Determining acceleration behavior, and developing models, which include the impact of various ATC temperature ranges, dwell times, and maximum temperatures.
- Comparing Sn-Pb, high Ag SAC alloys, Sn-Ag, and low Ag SAC variants under more benign accelerated test conditions to get a trend of acceleration factors for different alloys at conditions closer to field use.

Summary and Conclusions

This investigation focused on the thermal fatigue performance of solder joints made using three common BGA ball alloys: SAC105, Sn-3.5Ag, and SAC305. Accelerated thermal cycle (ATC) testing was performed using a 1.0-mm pitch, 676 PBGA daisy-chain test vehicle. The BGA packages with electrolytic Ni/Au-finished component pads were assembled to high temperature rated Cu-OSP coated printed circuit boards using SAC 305 solder paste. ATC testing was performed using in-situ electrical monitoring and the IPC-9701A TC1 condition of 0/100°C with 10-minute dwells (nominal). Three different electrical failure criteria were used in constructing the Weibull failure curves: 20% resistance rise, 500 Ω , and hard open (infinite resistance). The following conclusions were drawn from this study.

1. SAC105 ball with SAC305 paste has the lowest thermal fatigue resistance under the conditions tested, with Sn-3.5Ag and SAC 305 having similar and superior performance. Failures for all alloys were confirmed to be due to thermal fatigue in the bulk solder near the package pad.
2. Use of the IPC-9701A standard failure criterion of 20% resistance rise provides the most sensitive measure of failure among those studied. Failure was typically detected 200 to 500 cycles sooner than for the coarser criteria, though somewhat more scatter was evident. The two high resistance failure criteria gave very similar Weibull curves.
3. The relatively poor performance of the SAC105 ball alloy joints does not necessarily mean this alloy has insufficient thermal fatigue resistance for specific applications. Comparison of the data from the current study with those from an earlier one using the same test vehicle suggest that SAC105 ball alloy joints may perform worse than those with eutectic Sn-Pb solder; however, it is suggested that a direct comparison within the same study be performed to validate or invalidate this conclusion.
4. Areas for further study of the thermal fatigue performance of solder joints have been identified, including assessments of the impact of dopants, varying surface finishes, and the development of acceleration models.

Acknowledgements

The authors would like to thank Noel Hancock, Gilbert Mancillas, Dave Roche, and Al Saxberg of HP for laboratory assistance, and Michael Roesch of HP for management support.

References

- [1] A.Syed., et al., "Alloying Effect of Ni, Co, and Sb in SAC solder for Improved Drop Performance of Chip Scale Packages with Cu OSP Pad Finish," proceedings ECTC, p. 404 (2006).
- [2] X. J. Zhao, et al., "Improvement of Mechanical Impact Resistance of BGA Packages with Pb-free Solder Bumps," proceedings EPTC, p. 174 (2006).
- [3] P. Kim, et al., "Improvement of Drop Reliability in OSP/Cu Pad Finished Packages," proceedings EPTC, p. 168 (2006).
- [4] A. Syed, et al., "Effect of Pb free Alloy Composition on Drop/Impact Reliability of 0.4, 0.5 & 0.8mm Pitch Chip Scale Packages with NiAu Pad Finish," proceedings ECTC, p. 951 (2007).
- [5] R. S. Pandher, et al., "Drop Shock Reliability of Lead-Free Alloys – Effect of Micro-Additives," proceedings ECTC, p. 669 (2007).
- [6] H. Kim, et al., "Improved Drop Reliability Performance with Lead Free Solders of Low Ag Content and Their Failure Modes," Proceedings ECTC, p. 962 (2007).
- [7] D. Kim, et al., "Evaluation of High Compliant Low Ag Solder Alloys on OSP as a Drop Solution for the 2nd Level Pb-Free Interconnection," proceedings ECTC, p. 1614 (2007).
- [8] G. Henshall, et al., "iNEMI Pb-Free Alloy Alternatives Project Report: State of the Industry," proceedings SMTAI, p. 109 (2008).
- [9] G. Henshall, et al., "Addressing Industry Knowledge Gaps Regarding New Pb-Free Solder Alloy Alternatives," proceedings IEMT, p. B4.2 (2008).
- [10] J. Bath, et al., "Reliability Evaluations of Lead-Free SnAgCu PBGA676 Components Using Tin-Lead and Lead-Free SnAgCu Solder Paste," proceedings SMTAI, p. 891 (2005).
- [11] C. Shea, et al., "Low-Silver BGA Assembly Phase I – Reflow Considerations and Joint Homogeneity Initial Report," Proceedings IPC APEX (2008).
- [12] C. Shea, et al., "Low-Silver BGA Assembly Phase I – Reflow Considerations and Joint Homogeneity Second Report: SAC105 Spheres with Tin-Lead Paste," Proceedings SMTAI, p. 424 (2008).
- [13] J. Pan, "Lead-Free Liquidus Temperature Calculator," <http://www.calpoly.edu/~pan/LTCalculator.html> (2008).
- [14] S. Yoon, et al., "Effect of Stress Relaxation on Board Level Reliability of Sn Based Pb-Free Solders," proceedings ECTC, p. 1210 (2005).
- [15] J.-P. Clech, "Lead-Free and Mixed Solder Joint Reliability Trends," proceedings APEX, p. S28-3-1 (2004).
- [16] T. Bieler, et al., "Influence of Sn Grain Size and Orientation on the Thermomechanical Response and Reliability of Pb-free Solder Joints," proceedings ECTC, p. 1462 (2006).
- [17] S. Terashima et al., "Effect of Silver Content on Thermal Fatigue Life of Sn-xAg-0.5Cu Flip-Chip Interconnects," J. Electronic Materials, Vol. 32, no. 12 (2003).
- [18] P. Roubaud, et al., "Thermal Fatigue Resistance of Pb-Free Second Level Interconnect," proceedings SMTAI (2001)
- [19] Private conversation with A. Syed, Amkor Technology (2008).
- [20] R. S. Pandher and R. Healey, "Reliability of Pb-Free Solder Alloys in Demanding BGA and CSP Applications," proceedings ECTC, p. 2018 (2008).